Chemical Geology 527 (xxxx) xxxx

Contents lists available at ScienceDirect

Chemical Geology

journal homepage: www.elsevier.com/locate/chemgeo

Global climate control on carbonate weathering intensity

Jérôme Gaillardet[a,*], Damien Calmels[b], Gibran Romero-Mujalli[c], Elena Zakharova[d], Jens Hartmann[c]

[a] Institut de Physique du Globe de Paris (IPGP), Sorbonne Paris Cité, University Paris Diderot, CNRS, Paris 75231, France and Institut Universitaire de France.
[b] GEOPS, Univ. Paris-Sud, CNRS, Université Paris-Saclay, 91405 Orsay, France
[c] Institut für Geologie, Centrum für Erdsystemforschung und Nachhaltigkeit (CEN), Universität Hamburg, Bundesstraße 55, 20146 Hamburg, Germany
[d] LEGOS, Université de Toulouse, CNES, CNRS, IRD, UPS Toulouse, 14 avenue E. Belin, 31400 Toulouse, France

ARTICLE INFO

Keywords:
Carbonate
Weathering
pCO_2
Climate
Global
Ecosystem

ABSTRACT

Carbonate rocks are a peculiarity of the Earth relative to other planets in the solar system. Large terrestrial areas are covered by carbonate lithology, which actively reacts with atmospheric/biospheric CO_2. Although carbonate rocks represent a major component of the global carbon cycle, their intensity and rates of chemical weathering have been overlooked. In this study, we examine three global databases of rivers and springs draining carbonate regions under various climate conditions (from −15 °C to +30 °C). Using $Ca^{2+} + Mg^{2+}$ concentrations as a proxy, we show that carbonate weathering intensity depends upon land temperature according to a boomerang-type relationship, with maximum dissolution between 10 and 15 °C. We show that this pattern is primarily controlled by thermodynamics if we assume that the partial pressure of CO_2 in soil (pCO_2) increases from atmospheric-like levels under cold climate up to 100 times the present day atmospheric concentration under hot climate. The link between soil pCO_2 and land temperature is still not very well known, but by using three different published predictive soil pCO_2 vs. T curves, we show that the boomerang shape can be, at least qualitatively, reproduced.

This study shows that more data on carbonate weathering in various environments are needed to predict with more accuracy the role that carbonate lithologies and overlying ecosystems could play in the Anthropocene.

1. Introduction

Carbonate rocks cover approximately 10–12% of ice-free continental areas according to Ford and Williams (2013) not including the clastic rocks containing carbonate minerals. In large parts of the planet, such as the Mediterranean region, South China, Central Siberia and Northern America, limestone and dolostone are the dominant rock types. Geomorphologists have been interested in carbonate weathering for a long time and have reported a lot of carbonate dissolution rate estimates in different parts of the world, especially for the purpose of understanding the role of climate in karst landforms (Corbel, 1959; Drake and Wigley, 1975; Gombert, 2002; Bakalowicz, 2005; Gabrovšek, 2009 for a review). In the geochemical community, chemical weathering has received increasing interest over the last 20 years as its global role in the regulation of atmospheric and ocean composition and in the formation of soils serves as a crucial component in understanding and predicting Earth's climate dynamics. Yet, despite this growing interest, the weathering of carbonates has surprisingly attracted little attention both in terms of its mechanisms and global budget. This lack of interest most likely relates to the seminal idea that, over long periods of time (0.5 to 1 Myr timescale), carbonate weathering is not a significant contributor to changes in the amount of atmospheric CO_2 (Berner and Berner, 2012). This idea is based on Eq. (1) showing that the weathering reaction of carbonate on land is exactly compensated by the precipitation reaction in the ocean:

$$Ca_x, Mg_{1-x}CO_3 + CO_2 + H_2O = xCa^{2+} + (1 - x)Mg^{2+} + 2HCO_3^- \quad (1)$$

However, for a number of reasons listed below, carbonate weathering should play a significant role at both global and regional scales and at short and long timescales.

- Carbonate rocks and minerals weather quickly and are therefore very sensitive to any kind of perturbation, like in particular the rapid increase of CO_2 in the atmosphere due to anthropogenic emissions and land use changes. According to Lasaga (1984), at 25 °C, pH = 5, the dissolution of a spheric calcite mineral of 1 mm of diameter typically takes 10^{-1} year, while the dissolution of the most weatherable silicate mineral (anorthite) takes 10^2 years. Note that

* Corresponding author.
E-mail address: gaillardet@ipgp.fr (J. Gaillardet).

https://doi.org/10.1016/j.chemgeo.2018.05.009
Received 3 November 2017; Received in revised form 19 March 2018; Accepted 7 May 2018

the kinetics of dolomite dissolution is intermediate between that of calcite and anorthite and is on the order of a year. Based on the chemical composition of streams draining a single lithological type in France, Meybeck (1986) has shown that limestone weathers 10 to 20 times faster than granitic rocks.

- As a consequence, the global flux of carbon and calcium transported by rivers to the ocean due to carbonate weathering is important. Based on the inversion of chemical composition of the largest rivers, Gaillardet et al. (1999) have shown that 80% of the Ca, 60% of Mg and 40% of Sr reaching the sea each year are derived from limestone and dolostone weathering. The same study revealed that 0.29 Pg (10^{15} g) of carbon derived from carbonate weathering reactions are transported to the ocean each year. Based on Eq. (1), half of this number corresponds to CO_2 derived from the atmosphere, i.e. 0.15 PgC/year. This estimate does not take into account the small coastal areas and is probably underestimated. This represents about 6% of the flux of anthropogenic carbon sequestered in the global biomass or in the ocean in 2009 (Le Quéré et al., 2009) and is therefore significant.
- The carbonate reservoir is the largest carbon reservoir at the surface of the Earth along with the fossil organic carbon reservoir. Accumulating during the Earth's geological history (essentially during the Proterozoic era), its size is estimated between $50 \cdot 10^6$ and $120 \cdot 10^6$ PgC (Berner and Berner, 2012). For comparison, the amounts of C stored in the atmosphere and in the ocean are 720 PgC and 38,000 PgC respectively, i.e. at least 70,000 and 130 times lower. As a consequence, any imbalance, even small, in the carbonate reservoir between the input (carbonate precipitation by oceanic organisms) and outputs (chemical weathering and metamorphism) could have important transient consequences on the atmospheric CO_2 level.
- The weathering reaction written above (Eq. (1)) is not the only possible reaction and carbonate weathering can also occur due to acids other than carbonic acid. The weathering of limestones by sulphuric and nitric acids has been shown to occur in nature by several authors (Ebelmen, 1845; Spence and Telmer, 2005; Lerman and Wu, 2006; Calmels et al., 2007; Perrin et al., 2008). Sulphuric acid can be of natural origin (i.e. volcanic degassing followed by atmospheric oxidation, oxidative weathering of pyrite, etc.) or anthropogenic (acid rains due to coal combustion) as shown for example in South China by Xu and Liu (2007) and Li et al. (2008). Nitric acid is essentially of anthropogenic origin where it is generated by the transformation of ammonium into nitrate. In both cases (sulphuric and nitric acids), dissolved calcium is not simply compensated by just bicarbonate ions as assumed in Eq. (1), but can be coupled to other anions with the implication being that the reverse reaction (as in Eq. (1)) is not possible. Carbonate weathering by sulphuric acid can be written as follows:

$$2CaCO_3 + H_2SO_4 = 2Ca^{2+} + SO_4^{2-} + 2HCO_3^- \quad (2)$$

This reaction produces both sulphate and bicarbonates as compensating ions. As discussed in Calmels et al. (2007) for the Mackenzie basin, the different residence time in the ocean of sulphate and bicarbonate ions introduces an interesting decoupling with transient release of CO_2 in the hydrosphere-atmosphere system. Calmels et al. (2007) have shown that, for the Mackzenzie basin only, the flux of sulphate derived from oxidative weathering of sulphide (13 TgS/year) accounted for 28% of the global flux proposed by Berner (1984) suggesting that this latter value could be largely underestimated. At a global scale, the weathering of limestone by sulphuric acid is probably an underestimated process. The idea that chemical weathering of carbonates by sulphuric acid is a source of CO_2 to the ocean + atmosphere system was further exploited by Torres et al. (2014) to explain the relative stability of the partial pressure of atmospheric CO_2 during the Cenozoic. Recently, Torres et al. (2017) also proposed that carbonate weathering by sulphuric acid during glacial periods of the Quaternary was creating a negative feedback on the climate system by modulating atmospheric CO_2 levels.

These are some of the reasons suggesting that carbonate weathering is important for the Earth's surface regulation. The fast kinetics of carbonate weathering allows it to respond to changes at human timescales making it consequently an important component in future long-term climate models. As shown by the recent modeling paper from Beaulieu et al. (2012) in the Mackenzie river basin, in response to a doubling of atmospheric CO_2 levels, the increase in carbonate weathering would be responsible for 70% of the CO_2 consumption by rock weathering.

The aim of this publication is to report a global database on carbonate dominated rivers spanning all types of climates and to review the factors potentially controlling carbonate weathering intensity. We investigate the link between carbonate weathering intensity and climate (mostly temperature) and show that a relatively simple relationship exists between carbonate weathering intensity and land temperature. This bell-shaped relationship is proposed to result from the competition between thermodynamic control on carbonate weathering and the variability in soil CO_2 production by soil biota at the global scale. While this conceptual framework is able to reproduce qualitatively the trend observed at the global scale, other factors explaining the important variability of data must be accounted for. To our knowledge, this study is the first reporting a global database of well-selected rivers draining relatively pure carbonate rocks and aims at stimulating further studies on carbonate weathering fluxes and controls at the surface of the Earth.

2. Origin and selection of data

The map showing the carbonate dominated areas of the continents is given in Fig. 1. We have tried to select data from the different carbonate provinces of the world and from sites covering different climate types. We are naturally limited by the places of carbonate outcrops as well as by the limited number of published studies reporting all the required parameters.

First, a database was assembled by harvesting literature data for river waters draining pure carbonate rocks (see footnotes of Table 1) and applying a series of criteria (detailed below). Mixed lithologies such as marls, calcareous shales were avoided. Table 1 is based on data from France (Jura Mountains, Seine watershed, Herault watershed, French Alps); Slovenia, Russia (Crimea and Siberia); Taiwan; China (Sichuan and Guizhou provinces); Nepal; Thailand; Fly basin, Papua New Guinea, Congo basin, Puerto Rico, USA (Florida and Pennsylvania) and from Canada (NWT). When climate gradients were locally important, data were grouped and averaged by temperature range (Table 1 and Table S1). This database was completed by unpublished data of Russian rivers. These latter data were collected in data reports from the former USSR (in Russian) and averaged by location (annual averages for the years 1959, 1960, 1961 and 1962 for Chernaya, and 1957, 1961 and 1962 for Olenek in Table 1). Other unpublished analyses from central China are also displayed in Table 1 and Table S1. The Table 1 shows that the number of samples per locality is variable but usually small, with the exception of the Jura Mountains (Calmels et al., 2014). For each location and according to temperature ranges, Ca + Mg concentrations were calculated and averaged. Table 1 only gives the mean and standard deviation for each data population. The whole dataset can be found in Table S1 in the appendix. When not available in the source papers, mean annual surface temperatures were extracted from Hijmans et al. (2005).

In parallel, the GLORICH database was used to extract rivers dominated by carbonate sedimentary rocks using the criteria that are given below. The GLORICH database (Hartmann et al., 2014) reports raw data from the scientific literature, the USGS and national water agencies from North America, France, Germany, Spain, and South Africa. Only a few % of the data are common in Table 1 and the

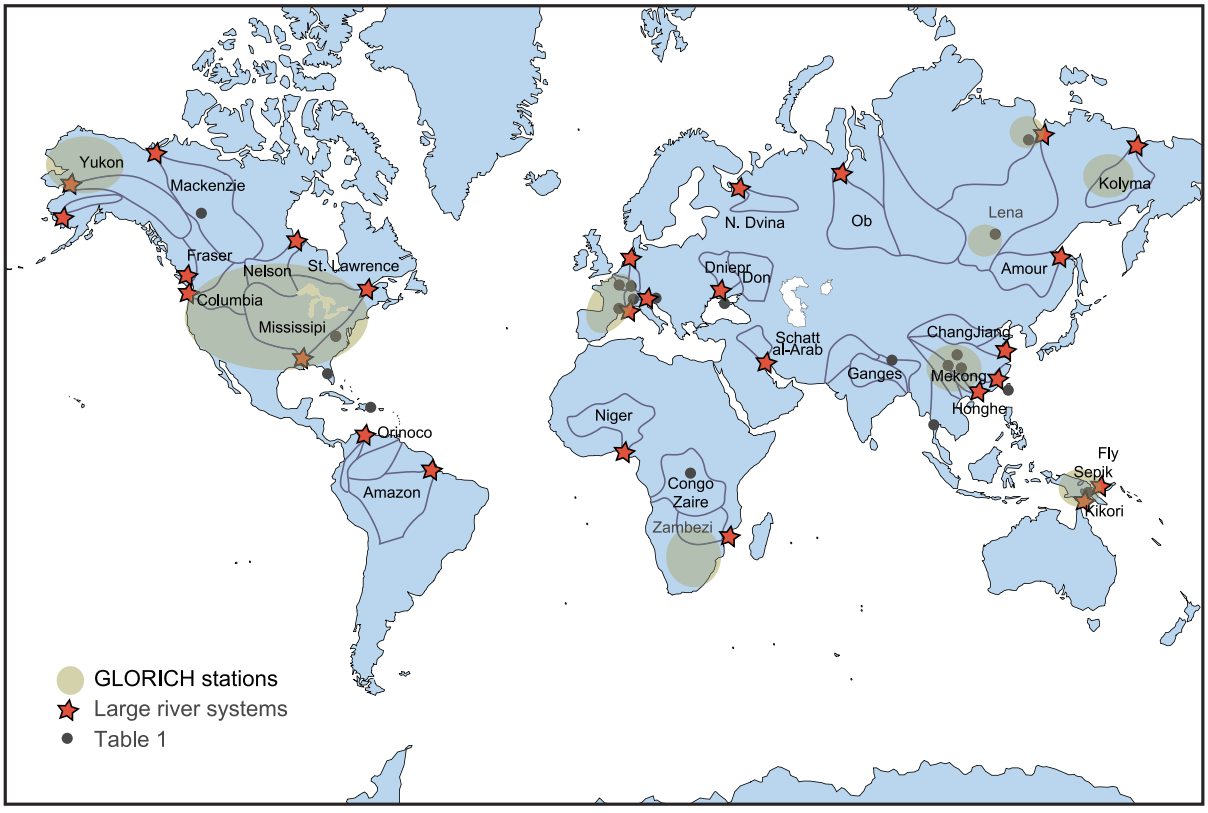

Fig. 1. Map of the data location. The three groups of data have been separated: GLORICH data (colored zones), data from Table 1 and selected large rivers from Gaillardet et al., 1999.

GLORICH database. As a consequence, while the database from Table 1 contains 26 averaged data, the GLORICH database contains 2781 data points corresponding to individual sampling dates. Instantaneous water discharge measured the day of sampling is reported for a number of catchments, essentially for locations in Northern America. No statistics were done on the GLORICH database, which is used here to illustrate the variability in Ca and Mg concentrations.

01 Finally, a third dataset was used focusing on the 60 largest rivers of the planet, corrected for rain, silicate weathering and evaporite dissolution. Proportions of major elements from these sources are derived from the mathematical inversion of large river geochemistry (Gaillardet et al., 1999). These large rivers cannot be directly compared to rivers and springs listed in Table 1 and the GLORICH database as they carry water that has drained various lithologies and not strictly carbonate rocks, but they will be used for comparison. We only selected the rivers for which the proportion of Ca from carbonate was higher than 75% to best avoid this "dilution" effect. Locations are shown in Fig. 1.

02 In order to gather and compare the different databases, we made sure that the selected rivers and springs were only draining pure carbonate lithologies (i.e. no evaporitic rocks or silicates), that atmospheric/soil CO_2 was the only significant acid providing protons for mineral dissolution and that the sites were not too much impacted by human activities. Although the subject is still a matter of debate, a couple of papers have shown that nitric acid, derived from nitrification processes, can provide protons and increase chemical weathering rates of carbonates (Perrin et al., 2008). Similarly, sulphuric acid formed by the action of oxygen on sedimentary sulphides (e.g., Calmels et al., 2007; Li et al., 2008) can also be a source of protons able to dissolve carbonates without the involvement of atmospheric/soil CO_2. As a consequence, a series of criteria was applied to the data in order to select the springs and rivers of interest for the purpose of this study. When necessary and when possible (when Cl concentration was available), data were corrected for sea salt inputs using seawater Cl-normalized ratios and assuming that Cl^- was only sourced from sea salt. For samples with relatively elevated Cl^- concentration, this correction only affected Na^+, Mg^{2+} and SO_4^{2-} concentrations (due to their relatively low Cl-normalized ratio in seawater) but never affected Ca^{2+}. In Table 1, this correction was only significant for Puerto Rico. The rivers were selected as follows:

- Only rivers with molar (Ca + Mg)/Na ratio higher than 10 were considered. This criteria was applied to include rivers influenced by dolostone dissolution and to discard rivers that may be impacted by silicate weathering (silicate dominated rivers have a much lower Ca/Na molar ratio, between 0.3 and 0.5, Negrel et al., 1993).
- Rivers with Cl/Na molar ratio higher than 2 as well as rivers with high nitrate concentrations (>100 µmol/l) were discarded to avoid any strong agricultural impact. Cl^- is often associated with fertilizer inputs and is therefore a good proxy for agricultural inputs (Roy et al., 1999; Floury et al., 2017).
- Rivers showing (Ca + Mg)/SO_4 < 10 were discarded due to potential influence of sulphide oxidation (providing H^+ ions) or gypsum dissolution (providing an excess of Ca^{2+}).

For the different databases used in this paper, we calculated and used Ca + Mg concentrations as a proxy for carbonate weathering intensity (Table 1). Calcite Saturation index (SIc) was computed by taking into account ionic strength and is listed in Table 1.

3. Results

The datasets used in this study cover a reasonable range of climate settings as illustrated in Fig. 1. The GLORICH database reports a high density of data from North America, Western Europe (mainly France), and South Africa and is therefore over-representing these regions of the word. Interestingly, the GLORICH database can be used to evaluate the

Table 1
Carbonate weathering intensities.

Region	T	Runoff	Ca + Mg	SIc	Reference
	°C	mm/yr	μmol/l		
Jura Mountains					(1)
Mean	6	1530	1711	0.50	
SD			220		
Jura Mountains					(1)
Mean	8	1190	2357	0.69	
SD			239		
Jura Mountains					(1)
Mean	10	955	2499	0.51	
SD			305		
Seine watershed					(2)
Mean	10	280	2540	0.82	
SD			324		
Hérault watershed					(3)
Mean	13	865	2219	0.19	
SD			327		
French Southern Alps					(4)
Mean	9	600	1654	0.64	
SD			485		
Slovenia					(5)
Mean	6	1520	1336	0.27	
SD			204		
Slovenia					(5)
Mean	8	1540	1738	0.46	
SD			513		
Slovenia					(5)
Mean	10	560	2256	0.41	
SD			335		
Crimea					This study
Mean	11		1936		
SD			69		
Olenek province					This study
Mean	−12		699		
SD			64		
Siberia					(6)
Mean	−7	110	1632	0.31	
SD			304		
Siberia					(6)
Mean	−14	150	842	0.32	
SD			344		
Taiwan					(7)
Mean	22	2200	1297	0.17	
SD			309		
Wujiang watershed					(8)
Mean	17	600	1943	0.97	
SD			318		
Dadu He watershed					(9)
Mean	6		1545	0.49	
SD			427		
Upper Minjiang watershed					(9)
Mean	12		1200	0.82	
SD			339		
Minjiang watershed					(9)
Mean	16		2107	0.84	
SD			683		
Guizhou Province					(10)
Mean	20		1701	0.62	
SD			205		
Guizhou Province					(11)
Mean	11		1514	0.03	
SD			26		
Guizhou Province					(11)
Mean	17		2551	−0.07	
SD			279		
Nepal					(12)
Mean	14		976	0.63	
SD			436		
Thailand					(13)
Mean	26	2300	1533	0.24	
SD			73		
Fly river watershed					(14)
Mean	28	4330	569	−0.44	
SD			108		
Congo watershed					(15)
Mean	25	550	1042		
SD			412		
Puerto Rico					(16)
Mean	24	900	1831	0.15	
SD			572		
Florida					(17)
Mean	20		1563	0.17	
SD			212		
Pennsylvania					(18)
Mean	9		2259	−0.20	
SD			562		
North Western Territories					(19)
Mean	−1	340	1213	0.14	
SD			558		

References: (1) Calmels et al. (2014). (2) Roy et al. (1999). (3) Petelet et al. (1998). (4) Sarazin and Ciabrini (1997). (5) Szramek et al. (2007). (6) Huh et al. (1998). (7) Yoshimura et al. (2001). (8) Han and Liu (2004). (9) Qin et al. (2006). (10) Xu and Liu (2007). (11) Li et al. (2008). (12) Oliver et al. (2003). (13) Pitman (1978). (14) Ferguson et al. (2011). (15) Negrel et al. (1993). (16) Giusti (1978). (17) Katz et al. (1998). (18) Jacobson and Langmuir (1974). (19) Millot et al. (2003). SIc, calcite saturation index $SIc = \log[(Ca^{2+})\cdot(CO_3^{2-})/Ks]$ where parentheses denote chemical activities and Ks is the solubility constant of $CaCO_3$ (supersaturation when SIc > 0).

variability of carbonate weathering intensity within a given climate zone.

Overall, Ca + Mg concentrations in rivers draining carbonate lithologies show a wide range of variability, ranging from about 500 μmol/l for the less concentrated waters of the Mackenzie river basin, Siberia, and Fly River basin to 3000 μmol/l in the temperate region of the Jura Mountains or in the temperate carbonate provinces of North America (Table 1).

Base cation concentrations (Ca + Mg) from the different databases are reported in Fig. 2 as a function of mean annual air temperature. Mean annual air temperature does not necessarily represent the effective temperature of water-rock interaction, which is more difficult to estimate, but is considered here as a climate proxy. Clear overall patterns of carbonate weathering intensity with temperature emerge, despite the large variability associated with each temperature range. Carbonate weathering intensity, as represented by Ca + Mg concentrations, is maximum for temperature between 5 and 15 °C, corresponding to rivers from the temperate zone. This bell-shaped relationship of carbonate weathering intensity as a function of temperature is visible on the three sources of data compared here (Table 1, GLORICH data and large river data). At lower and higher temperatures, Ca + Mg concentrations decrease. This decrease is approximately 120 μmol/°C between 10 °C and 25 °C for the three datasets. Below 10 °C, the rising part of the boomerang has a variable slope depending upon the dataset considered (110 μmol/°C for the GLORICH database to 60 μmol/°C for the Table 1 and for the large rivers). However, it is important to keep in mind that the density of data is lower at low temperatures than at temperatures higher than 10 °C.

The GLORICH data show that the variability at a given temperature is important. For example, within the temperate zone Ca + Mg concentrations can vary between 1500 and 3000 μmol/l, probably depending upon hydrological conditions and/or local geomorphic or environmental specificities. We plotted in Fig. 3 the carbonate weathering intensity as a function of runoff (discharge at the sampling date normalized to drained surface area) for a few catchments from the GLORICH database – those having >50 observations and instantaneous water discharge record – and also for rivers from Slovenia (Szramek et al., 2007). Fig. 3 shows generally that, with increasing runoff,

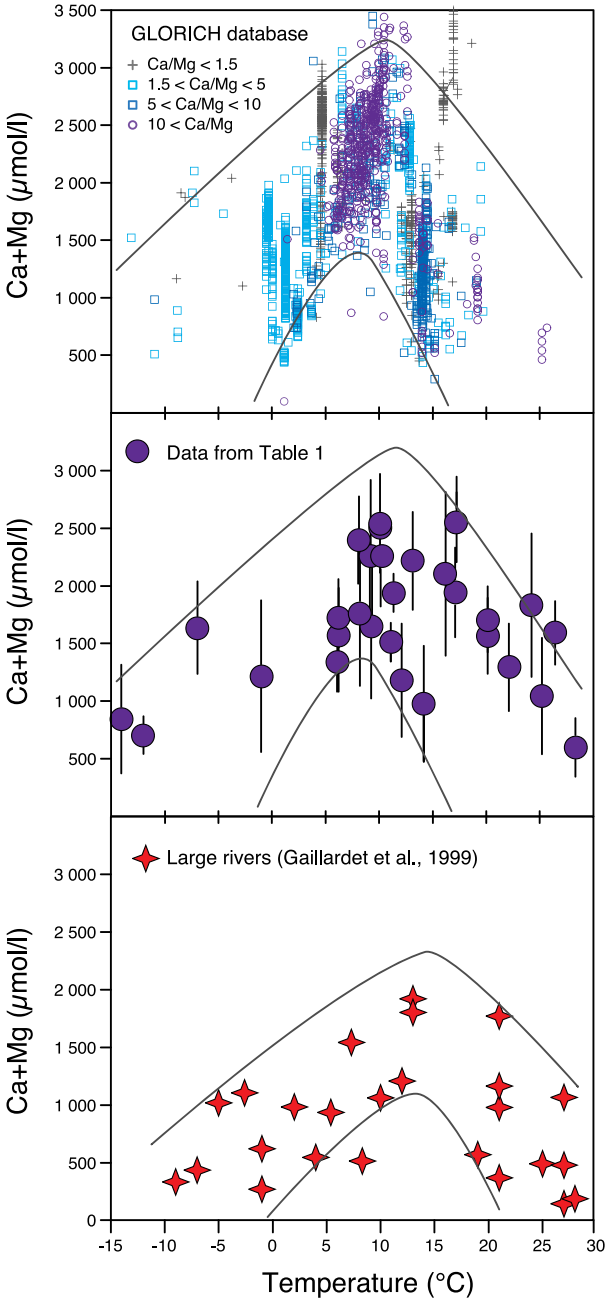

Fig. 2. Carbonate weathering intensity as indicated by Ca + Mg concentrations in the three database investigated in this paper as a function of air temperature. Panel a: GLORICH database (ref); Panel b: data from Table 1; Fig. 3a: Large river data after mathematical inversion (Gaillardet et al., 1999). All database display a boomerang-shape curve indicating that carbonate weathering is maximum under temperate climate. In Panel a, color code indicates different classes of Ca/Mg ratios. In Panel b, error bars are standard deviation on the mean value.

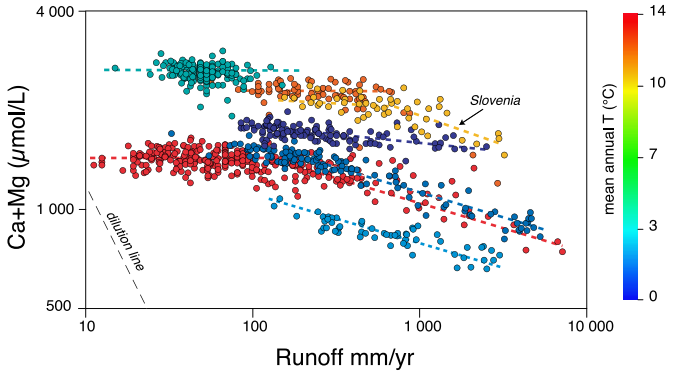

Fig. 3. Log-Log relationship between weathering intensity and instantaneous water discharge normalized to catchment surface area for rivers from the GLORICH database and from Slovenia (Szramek et al., 2007) color-coded for mean annual temperature. This figure illustrates the chemostatic behavior of carbonate dominated rivers, i.e. the non-dilution for concentrations with increasing discharge. A pure diluting behavior would follow a slope of −1 in this diagram indicated by the dashed line. For individual events associated to high discharge, concentrations decrease significantly, explaining part of the variability of carbonate weathering intensity at a given temperature.

5-6
2 notes:

concentrations are not following a pure dilution trend (in runoff^{-1}) and either remain constant over the whole range of discharge or slightly decrease after a given catchment-specific threshold. Fig. 3 confirms the chemostatic behavior of carbonate-dominated rivers already pointed out by Bluth and Kump (1994) or Zhong et al. (2017) and suggests that part of the variability observed in the GLORICH database (and by extension in the three databases) at a given temperature can be due to hydrological factors.

The GLORICH data also allows us to investigate the effect of the composition of carbonate bedrock on their dissolution intensity. From the data (n = 2762), 538 samples have Ca/Mg lower than 1.5 and are therefore impacted by dolomite dissolution whereas 561 samples have Ca/Mg higher than 10 and are therefore draining pure Ca-carbonates. On Fig. 2, it seems that a Ca/Mg ratio of 1.5 represents a threshold value above which carbonate weathering intensity follows the general boomerang curve and below which the pattern of weathering intensity with temperature is more erratic. It is also interesting to note that none of the databases considered in this paper exhibit Ca-rich springs and rivers at low temperature, suggesting either that Ca-rich limestones are rare at high latitude or that there are mechanisms removing Ca from river and spring waters in low temperature zones (e.g., freezing).

Finally, large rivers also exhibit a bell-shaped pattern in the (Ca + Mg) vs. air temperature space. This pattern appears to be shifted to lower values when compared to the data from Table 1 and from GLORICH. This is easily understandable as these concentration, calculated from an inverse model, do not take into account the "dilution" effect due to the fact that large rivers collect water draining all lithologies and not only carbonate lithologies. This is particularly true for the tropical silicate-dominated rivers such as the Zaire and Amazon rivers whose drainage catchment is poor in carbonate formations.

4. Discussion

In the following discussion, we propose that the shape of the boomerang relationship observed between carbonate weathering intensity and mean annual temperature at the global scale is mostly due to the availability of soil CO_2 for weathering reactions. We first examine what should be expected from a theoretical point of view using a thermodynamic approach and then shift to the role of CO_2 production in soils on carbonate weathering intensity.

4.1. Thermodynamic approach

Carbonate minerals dissolve congruently and are characterized by rapid kinetics of dissolution. Carbonate dissolution kinetic data indicate that equilibrium or near-equilibrium conditions are reached between calcite and water within a couple of hours (Dreybrodt, 1988; Dreybrodt et al., 1996; Eisenlohr et al., 1999). Assuming dissolution of pure calcite or aragonite at equilibrium, i.e. considering Mg^{2+} as an ion non-involved in carbonate weathering, the dissolution of carbonate is governed by the following equations:

7-8
2 notes:

$$CaCO_{3(s)} = Ca^{2+}_{(aq)} + CO^{2-}_{3(aq)} \quad (3)$$

$$HCO^{-}_{3(aq)} = CO^{2-}_{3(aq)} + H^{+}_{(aq)} \quad (4)$$

$$CO^{*}_{2(aq)} + H_2O_{(l)} = HCO^{-}_{3(aq)} + H^{+}_{(aq)} \quad (5)$$

$$CO_{2(g)} = CO^{*}_{2(aq)} \quad (6)$$

$$H_2O_{(l)} = H^{+}_{(aq)} + OH^{-}_{(aq)} \quad (7)$$

09
cholas Gubbins

For each of these equations, a mass action law can be written:

$$(Ca^{2+})\cdot(CO_3^{2-}) = Ks \quad (8)$$

$$\frac{(CO_3^{2-})\cdot(H^{+})}{(HCO_3^{-})} = K_2 \quad (9)$$

$$\frac{(HCO_3^{-})\cdot(H^{+})}{(CO_2^{*})} = K_1 \quad (10)$$

$$K_H = \frac{(CO_2^{*})}{(pCO_2)} \quad (11)$$

where Ks is the solubility product of $CaCO_3$, K_2, K_1 and K_H, the equilibrium constants of Eqs. (4), (5) and (6) - also called the Henry's constant. Parentheses denote chemical activities and pCO_2 is the partial pressure of CO_2 in equilibrium with the solution. As in nature, the fluids interacting with limestones are not pure, the activity coefficient must be introduced to relate concentrations to activities. We denote γ_1 and γ_2 as the activity coefficients for single-charged and double-charged species respectively. These coefficients can be calculated using Davies equation:

$$\log(\gamma) = -Az^2\left(\frac{\sqrt{I}}{1+\sqrt{I}} - 0.3I\right) \quad (12)$$

where A is a temperature related constant, z is the charge of the chemical species and I is the ionic strength of the solution.

In addition, electro-neutrality of a fluid composition imposes that

$$[H^+] + [Na^+] + [K^+] + 2[Ca^{2+}] + 2[Mg^{2+}] = [Cl^-] = 2[SO_4^{2-}] + [NO_3^-] + [HCO_3^-] + 2[CO_3^{2-}] + [OH^-] \quad (13)$$

By grouping the species with no acid-base behavior (or conservative with regards to pH) and neglecting H^+, OH^- and CO_3^{2-} concentrations (the solution pH is expected to be between 6.5 and 8.5), we can write that

$$2[Ca^{2+}] = [HCO_3^-] + Rb \quad (14)$$

with $Rb = [Cl^-] + 2[SO_4^{2-}] + [NO_3^-] - [Na^+] - [K^+] - 2[Mg^{2+}]$ being the reduced alkalinity (Michard, 2002).

In order to predict the concentration of Ca in the interacting solution, two ideal situations can be distinguished (Garrels and Christ, 1965; Michard, 2002). The first case scenario, the open system, assumes that the solution reaches equilibrium with calcite at constant pCO_2. Assuming that Rb is close to 0 (i.e. the solution only contains the ionic species Ca^{2+}, HCO_3^-, CO_3^{2-}, H^+ and OH^-), the calcium concentration can be predicted as:

$$[Ca^{2+}] = \left(\frac{K_1K_HK_S}{4K_2\gamma_1^2\gamma_2}pCO_2\right)^{\frac{1}{3}} \quad (15)$$

The second working hypothesis consists of a closed system dissolution scenario, in which the solution first equilibrates with a given soil pCO_2, then continues to moves downward (and isolating itself from the source of CO_2) and finally starts dissolving calcite. A new set of equations can be written to calculate equilibrium Ca concentration resulting from calcite dissolution in a closed system:

$$K_H = \frac{(CO_2^{*})_0}{(pCO_2)_0} \quad (16)$$

where the subscript 0 denotes the initial conditions (for example in the upper soil layer) before calcite dissolution.

A supplementary equation can be written, expressing the conservation of all carbon species by introducing ΣC, the total dissolved inorganic carbon.

$$\Sigma C = [H_2CO_3] + [HCO_3^-] + [CO_3^{2-}] = [CO_2^*]_0 + [Ca^{2+}] \quad (17)$$

because the dissolution of 1 mol of calcite releases 1 mol of C to the solution. Eq. (17) can be simplified for pH lower than 8.5 and becomes:

$$[CO_2^*]_0 + [Ca^{2+}] = [CO_2^*] + [HCO_3^-] \quad (18)$$

Then, under the closed system assumption and neglecting Rb, the predicted Ca concentration can be solved numerically using the following equation:

$$[Ca^{2+}]^3 + \frac{K_1K_S}{4K_2\gamma_1^2\gamma_2}[Ca^{2+}] - \frac{K_1K_HK_S}{4K_2\gamma_1^2\gamma_2}(pCO_2)_0 = 0 \quad (19)$$

Calculations at equilibrium were performed using PHREEQC software and "phreeqc.dat" database (Parkhurst and Appelo, 1999).

For the two working models (open and closed systems), calculations have been conducted by assuming Rb = 0. Table 1 shows that Rb can be positive or negative. For instance, in the Jura Mountains where Ca ≫ Mg, Rb generally varies between −200 and +200 µequ/l. The effect of Rb is to increase the HCO_3^- concentration at equilibrium. Predicted Ca concentrations will be lower when Rb is close to 0 than when Rb is positive or negative. We checked using PHREEQC that if Rb varies between −200 and +200 µequ/l, the propagated variations on Ca concentration at equilibrium are within 5%. Reaction constants and standard enthalpies are given in Table 2.

4.2. Temperature effects

In open and closed systems, the control of temperature on Ca concentration in solution at equilibrium with respect to calcite can be predicted based on Eqs. (15) and (19), in which each thermodynamic constant has a temperature dependence. The effect of temperature, T, at constant pCO_2 and total pressure can be calculated based on the van't Hoff equation:

$$\frac{d(LnK)}{dT} = \frac{-\Delta H_0^{react}}{RT^2} \quad (20)$$

with K being the reaction constant, ΔH_0^{react} the standard enthalpy of the reaction and R the gas constant. Reaction enthalpies, taken from Parkhurst and Appelo (1999), show that K_1 and K_2 increase with temperature (Table 2) but that K_s and the Henry's constant for carbonic acid decreases with temperature. It is known that cold water is prone to dissolve more CO_2 than warm water. Amongst the four thermodynamic constants utilized in the calculation of equilibrium Ca concentrations, Henry's constant shows the strongest temperature dependency. Calculations (Fig. 4) show that in both open and closed system conditions, Ca concentration decreases with increasing temperature and hence that calcite dissolution is favored at low temperature. From 0 °C to 30 °C, the

Table 2
Mass action law constants at 25 °C and reaction standard enthalpy (ΔH_r°) for the reactions listed in the text.

Reaction number	Constant name (K)	Constant	ΔH_r° (kJ mol^{-1})
3	K_s	$10^{-8.48}$	−9.61
4	K_2	$10^{-10.329}$	14.90
5	K_1	$10^{-6.352}$	9.109
6	K_H	$10^{-1.468}$ [a]	−19.983
7	K_e	10^{-14}	55.9066

Thermodynamic data was taken from phreeqc.dat (Parkhurst and Appelo, 1999).

[a] Henry's constant for dissolution of gas CO_2 in water.

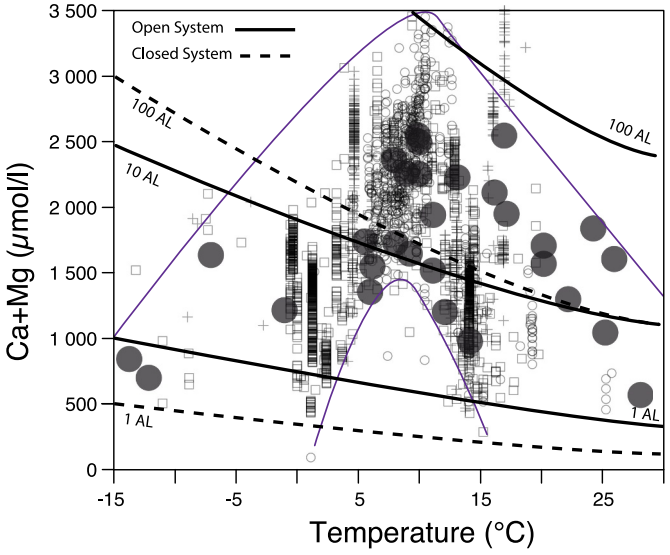

Fig. 4. Predicted effect of temperature on Ca + Mg concentrations at thermodynamic equilibrium and using temperature dependence of the reaction constants of the different chemical reactions of calcite dissolution. Open and close systems conditions are compared.

predicted Ca concentration in an open system varies by about −50 µmol/°C, −30 µmol/°C and a few µmol/°C for equilibrium pCO_2 equal to 100, 10 and 1 times the atmospheric value (390 ppmV in 2002) respectively, showing that the temperature effect on the Henry's constant is dominant. In closed system conditions, variations of Ca concentration with temperature are weaker due to the lesser importance of CO_2 dissolution. Clearly, the predicted concentration patterns as a function of temperature do not reproduce the boomerang relationship observed in the natural data. Moreover, it is obvious that only the open system conditions between 10 and 100 times atmospheric pCO_2 are compatible with the order of magnitude of Ca and Mg concentrations measured in springs and rivers draining limestone (Fig. 4). The closed system model would need unrealistic pCO_2 to explain the highest concentrations observed in the temperate regions. Considering the uncertainties of the above calculations (we assume here dissolution of pure calcite but the presence of Mg can change the solubility constant), and the data variability, we considered that the information on the slope is more relevant than that of concentration and conclude that carbonate weathering intensity (as recorded in Ca + Mg concentrations) is compatible (for temperature higher than 10 °C) with a temperature control at thermodynamic equilibrium but only at relatively high pCO_2. Overall, the misfit between data and a temperature-based model for carbonate dissolution shows that other parameters than temperature must play a role.

4.3. Effect of soil partial pressure of CO_2

As suggested by Eqs. (15) and (19), temperature is not the only parameter that controls predicted Ca concentration, which also depends upon pCO_2 that equilibrates (initially or continuously) with the water. If we assume that most of carbonate weathering occurs in soils where pCO_2 is elevated due to biological production (Drake, 1980; Drake and Wigley, 1975), then the prediction of carbonate dissolution as a function of temperature is more complicated than a simple effect of temperature on thermodynamic constants. In fact, temperature also affects the production of biogenic CO_2. Biogenic CO_2 is produced by both root respiration and soil organic matter decomposition by microorganisms. High temperature is typically more favorable to organic matter decomposition than low temperature. In addition, the physical properties (porosity and permeability) of soils, soil moisture and hydrology are key factors that drive the diffusion of soil CO_2 to the atmosphere and in a sense the amount of CO_2 that can be dissolved in soil pore water.

In the following section, we propose to use different estimates of pCO_2 in global soils.

A first approach is to scale the production of soil CO_2 to net primary production (NPP, the amount of organic matter in g of dry matter/m^2 fixed by the ecosystem). CO_2 is produced in the soil by heterotrophic and autotrophic respiration. Gwiazda and Broecker (1994) estimated that the production of soil CO_2 in the root zone corresponds to 75% of the NPP. If we assume that soil T controls the NPP, which in turns controls soil pCO_2, it is possible to derive a relationship between soil pCO_2 and temperature. The variation of NPP with land temperature was calculated using the Lieth (1975) relationship:

$$NPP = 3000/(1 + e^{1.315-0.119.T}) \quad (21)$$

where T is the land temperature in °C. As developed in Gwiazda and Broecker (1994) and more recently by Goddéris et al. (2009 and 2010), pCO_2 can be derived by solving the CO_2 diffusion equation in soil (initially from Van Bavel, 1951) that depends upon the diffusion of gaseous CO_2 in the air, soil porosity, tortuosity and temperature. Assuming that the maximum of CO_2 is generated at the mean root depth, we used the values recommended by Goddéris et al., 2010 and calculated soil pCO_2 as a function of T as follows:

$$pCO_2 = pCO_2atm + \frac{A.\ 0.75.\ NPP}{T^2} \quad (22)$$

with $A = 1.03 \cdot 10^6$ and T expressed in K.

A second approach consists of using the work of Brook et al. (1983). The authors compiled mean growing season soil pCO_2 for 19 regions of the world covering the whole range of climatic conditions and established, through bivariate and regression analysis, empirical relationships between log(pCO_2) and temperature, evapotranspiration rate and precipitation rate. We plotted Brook et al. (1983) pCO_2 data as a function of temperature and fitted the data using a logistic function (Eq. (23); Fig. 5). The obtained equation is as follows:

$$\log_{10}(pCO_2) = \log_{10}(pCO_2atm) + \frac{1.5}{(0.75 + e^{-0.12.T})} \quad (23)$$

where pCO_2 trends toward atmospheric values when T decreases and toward $10^{-1.5}$ atm at high temperatures.

Finally, the last approach consists in using the recent estimate of soil

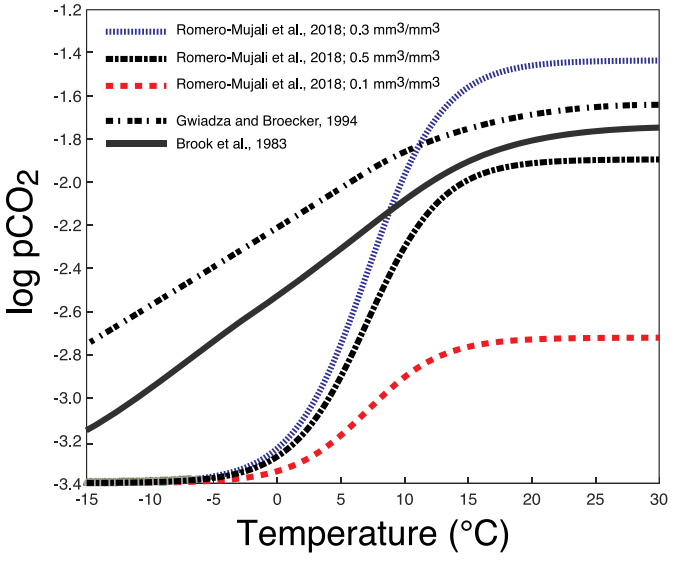

Fig. 5. Predicted soil Partial pressure of CO_2 (pCO_2) as a function of temperature for the three scenarios considered in this study. Soil pCO_2 calculated by Romero-Mujalli et al. (2018) are shown for three contrasted soil humidity values (0.1 mm^3/mm^3, 0.5 mm^3/mm^3, 0.3 mm^3/mm^3).

pCO_2 from Romero-Mujalli et al. (2018) that proposed the following control for soil pCO_2:

$$\log_{10}(pCO_2) = \log_{10}(pCO_2 atm) + \frac{e^{\left(-3\theta - \frac{0.25}{\theta}\right)}}{(0.09 + e^{-0.34.T})} \quad (24)$$

with θ the soil volumetric water content (m^3/m^3).

The different pCO_2 curves calculated using the three methods are plotted on Fig. 5 as a function of T. They all show that soil pCO_2 increases with temperature. Fig. 5 also shows that soil humidity can drastically affect soil CO_2. As reviewed by Romero-Mujalli et al. (2018) and Seneviratne et al. (2010), soil water content plays an important role in catchment energy and water balance at the Earth's surface. Soil moisture affects microbial metabolism and the gas exchanges (oxygen and carbon dioxide) at the ground-atmosphere boundary. Low soil water content limits the growth rate of plants and therefore the biological activity in the soil (Ilstedt et al., 2000), and also favors the diffusion of soil CO_2 to the atmosphere. Romero-Mujalli et al. (2018) showed that the pCO_2 in soils is optimal for θ value between 0.2 and 0.3 m^3/m^3.

Based on the above three soil pCO_2 patterns with temperature, the Ca concentration at equilibrium in closed and open systems can then be calculated based on Eqs. (15) and (19). Between −15 °C and 0 °C, the thermodynamic constants were calculated using a constant temperature of 1 °C to account for the absence of liquid water below this temperature. The different curves corresponding to the different scenarios are plotted on Fig. 6 for open system conditions. Results show that the general shape of the boomerang relationship is reproduced with steeper slopes for T < 15 °C than for T > 15 °C. At a first order interpretation, it is reasonable to propose that the boomerang pattern observed for global carbonate dissolution intensity with temperature results from two competitive mechanisms: the influence of temperature on the thermodynamic constants of the carbonate system and the global production of soil CO_2 by ecosystems. The increase in T favors both a decrease in carbonate weathering intensity due to the rapid decrease of the Henry's constant with T, and an increase in carbonate weathering intensity as soil pCO_2 globally increases with land T.

In details, none of the chosen curves for soil pCO_2 are able to explain the whole dataset. The Brook et al. (1983)'s soil pCO_2 prediction does show a bell-shape curve with maximum Ca + Mg concentrations found around 15 °C in agreement with the data but fails to explain the highest temperature values. The NPP-controlled CO_2 curve (Gwiazda and Broecker, 1994) also reproduces a boomerang shape and shows a maximum carbonate weathering intensity at similar temperature than the river and spring datasets. However, it fails to quantitatively explain the observed concentrations at low and high temperatures. At cold and warm climates, soil pCO_2 predicted by Gwiazda and Broecker (1994) is too high to explain the low Ca + Mg concentrations found in carbonate draining rivers. A better prediction, at least in terms of shape, is done by the Romero-Mujalli et al. (2018)'s curves at high temperature. The slope of the Ca + Mg increase with temperature (between 0 °C and 15 °C) is well explained by the cases where soil moisture is between 0.3 and 0.5 mm^3/mm^3, despite the fact that the rise of CO_2 with T starts "too late" compared to what is needed to explain the data. In addition, Fig. 6 shows that whatever the soil humidity value is, the modeled slope of the Ca + Mg vs. T decrease is too weak compared to the data. The only possibility to explain the 120 μmol/°C decrease between 10 and 25 °C is to invoke a change in soil moisture in addition to temperature changes.

According to this very simple and qualitative interpretation, the bell-shaped curve of global carbonate dissolution intensity with temperature (Fig. 6) results from the competitive effects of thermodynamic and biospheric production of soil CO_2.

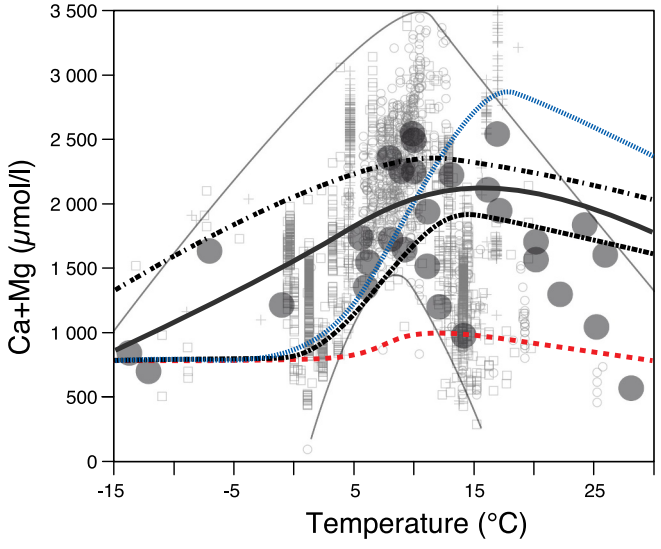

Fig. 6. Predicted Ca + Mg concentrations as a function of air temperature according thermodynamic equilibrium and using temperature dependence of the reaction constants and three different estimates of soil pCO_2 (Gwiazda and Broecker, 1994; Brook et al., 1983 and Romero-Mujalli et al., 2018) with contrasted soil humidity values. Only the case of an open system is considered. See Fig. 5 for legend. The data from the GLORICH database and from Table 1 are superimposed for comparison with the model curves.

4.4. The Jura case and the role of soil properties

In a previous study, we exemplify the role of ecosystem respiration processes on carbonate weathering on a study case in the Jura Mountain, France (Calmels et al., 2014). The Jura dataset is one of the datasets used in this paper. The Jura Mountain is a foreland alpine carbonate range from Central Europe showing a climatic (and superimposed ecological) gradient from the plains to the Mountain ridges. Calmels et al. (2014) have shown that carbonate weathering intensity along this gradient varies by a factor of 2.5 between 300 m and 1200 m elevation. Using a coupled ecological and hydrological model run on the two years of the sampling period (the ASPECTS model, from Rasse et al., 2001), Calmels et al. (2014), showed that the weathering intensity gradient can be explained by changes in vegetation types and soil properties. The ASPECT model uses hourly meteorological data (air relative humidity, air T, precipitation, global radiation, and wind velocity). According to the model, under a deciduous forest, the CO_2 produced by soil respiration (autotrophic and heterotrophic respiration) is on average higher than that produced in the coniferous altitude forest. The reason is that at low temperature, organic matter is less respired and organic matter accumulates in the soil. Despite important variations with time as a function of meteorological variability, on average, the soil pCO_2, in mountains is three times lower than in the plains. Soil structure impacts porosity and thus soil moisture. The Jura mountain study case shows that the production of soil CO_2 is the dominant process controlling carbonate weathering intensity at a regional scale and that this process can be affected by a number of potentially controlling factors such as the nature of organic matter and thus of the type of species and their physiology, soil properties and soil hydrology. Will all factors being constants, porosity and its distribution may favor CO_2 escape to the atmosphere or conversely its dissolution into soil pore water to produce carbonic acid. The Jura case, where these factors have been incorporated into a complex eco-hydrological model, shows that they should also play a role at the global scale and that soil humidity, which depends on precipitation rates, wind velocity, soil porosity and texture, T, and plant transpiration, should be an important parameter to take into account. The variability of soil properties and vegetation species at the global scale may explain the difficulty of our first order approach to explain correctly the slopes of the boomerang curve presented above.

4.5. Other factors influencing carbonate weathering

There are a number of other factors that may play a role on carbonate weathering intensity and therefore complicate the simple interpretation that we propose to explain the general bell-shape relationship between carbonate weathering intensity and temperature at the global scale. These factors may also contribute to the wide range of scatter which is observed when global databases are plotted as a function of temperature (Fig. 2).

- A quite evident controlling factor is carbonate composition. All the above calculations were made using the calcite dissolution equation and equilibrium constant, but the presence of Mg in almost all natural sedimentary carbonates (and other impurities) may lead to different Ks values. It is well known that the Ca/Mg ratio of seawater has changed through time (Holland, 2003), but information on the weatherability of limestones as a function of Ca/Mg ratios is still lacking. It should be kept in mind that when comparing the thermodynamic model developed above with data, we are making the hypothesis that real limestones behave like pure calcite.
- The hydrological factor is also potentially an important one as hydrological conditions can create departure from thermodynamic equilibrium by diluting, for example, concentrations. In particular, when temperature increases, runoff increases and tends to dilute rivers. Waters may then not be at saturation with respect to calcite and controlled by kinetic laws rather than mass action laws. This would lead to riverine concentrations lower than that expected at saturation (Maher and Chamberlain, 2014). The rivers characterized by high temperature would therefore be kinetically-controlled rather that thermodynamically controlled. However, except for the Fly watershed and water from Pennsylvania, all carbonate draining waters reported here are oversaturated with respect to calcite having calcite saturation indices (SIc) > 0 (Table 1). Despite the uncertainty mentioned above on the real Ks value, the hypothesis of a kinetic effect leading to low Ca + Mg concentrations in carbonate draining rivers is not supported by the data. As shown in Fig. 3, Ca and Mg concentrations are remarkably constant (chemostatic) with increasing runoff in carbonate-dominated rivers, a property illustrating the fast kinetics of carbonate dissolution. However, at high runoff concentration values tend to slightly decrease possibly because of the mixing of groundwaters with waters rapidly infiltrating. The calculation of the SIc for each samples plotted in Fig. 3 indicates that SIc is >0 for most the samples lying on the plateau but becomes <0 for the highest runoff values where Ca + Mg concentrations decrease. It is beyond the scope of the present paper to investigate in detail the concentration-discharge relationships in carbonate dominated rivers, but a more in-depth analysis on the links between travel times of water in the karstic system (and flowpath length) and equilibrium times, such as the recent study on silicate-dominated rivers by Ibarra et al. (2017) would clearly be illuminating. Hydrologic conditions could also influence carbonate dissolution by affecting the closed or open system conditions, with the possibility that higher runoff associated to higher hillslope hydraulic gradients and shallower water tables might change the system from open to close conditions. We observe from our dataset that mountainous rivers tend to have lower weathering intensities than rivers from the lowland, suggesting a potential control by hydrological factors. We did not find however any relationship between the mean slope and the carbonate weathering intensity for the different data bases used in this paper.
- Another source of variability in Ca + Mg concentrations could be the precipitation of secondary carbonates. During carbonate dissolution water equilibrates with higher pCO_2 (in soils) than in the atmosphere, and when water starts to be in contact with the atmosphere during its transfer from the hydrological system to the ocean, dissolved CO_2 tends to leave solution (Raymond et al., 2013). This CO_2 degassing leads to an increase in pH which then subsequently promotes carbonate precipitation. Carbonate precipitation would thus result in a decrease in Ca concentration. This degassing effect would be more pronounced for rivers draining high T regions because waters have originally equilibrated with higher soil pCO_2 than in low-T regions (see Fig. 5). The degassing (and thus carbonate precipitation) would then be dependent on the difference between aqueous pCO_2 (acquired in soils) and atmospheric pCO_2. This difference is much higher in high-T regions than in low-T regions, which might explain part of the low Ca + Mg concentrations observed at high T.
  At low T, the enrichment in Mg that is visible in Table 1 and in the GLORICH database (Fig. 2) may be an indication of secondary calcite formation. In cold climates, freezing could be a mechanism responsible for the precipitation of Ca-carbonate and thus a lowering of Ca concentration in residual water (Jessen et al., 2014; Thomazo et al., 2017). The formation of so-called “cryogenic calcites” could explain part of the depletion of Ca observed in the low-T regions. Very little is known about the importance of this process in high-latitude regions.
- Higher carbonate weathering intensities could be caused by additional sources of protons to the rivers. Many sources are possible with volcanic or metamorphic CO_2 being a possibility. It has been shown in many places that the passive degassing of metamorphic (Evans et al., 2004) and volcanic (Chiodini et al., 2001; Rive et al., 2013) CO_2 occurs. By reaching the soil, this deep source of CO_2 dissolves in water and constitutes an additional source of protons. Carbon isotopes could be used to help constraining the origin of the CO_2, but are rarely measured. In addition, river degassing fractionates carbon isotopes and complicates their interpretation in terms of sources. If the input of volcanic or metamorphic carbon can be considered as a source of additional acidity at the local scale, its role at the global scale is less plausible as most of the carbonate dominated regions investigated here (from GLORICH and Table 1) are in tectonically inactive regions (with the exception of Nepal, Taiwan and South China rivers). Another source of acidity that can be provided in many regions of the world is sulphuric acid, which is typically generated by sulphide oxidation. Although only rivers with Ca + Mg/SO_4 > 10 were selected, the influence of sulphide oxidation on Ca + Mg concentrations cannot be completely avoided. Sulphuric acid contribution to carbonate weathering has been demonstrated in a number of regions, such as South China (e.g. Li et al., 2008), Northern Canada (Calmels et al., 2007) and the Himalayas (Galy and France-Lanord, 1999; Karim and Veizer, 2000). In South China, Li et al. (2008) had shown that 42% of the carbonate dissolution in the karstic province of Guizhou was due to sulphuric acid sources. However, from the investigated database, no relationship between Ca + Mg concentrations and SO_4 concentration or Ca/SO_4 was found with temperature, indicating that a control of carbonate dissolution by sulphuric acid addition is very unlikely.
  Finally, another possible source of acidity is provided by nitric acid (generated by nitrification processes). It has been shown by Perrin et al. (2008) that in some agrosystems, a significant part of carbonate dissolution might be due to protons coming from the transformation of ammonium into nitrate. The application of fertilizers, particularly in temperate regions, may also be an additional factor explaining the variability of Ca + Mg concentrations. Because polluted rivers were discarded, and in the absence of significant correlation between Ca + Mg and NO_3 concentrations in the database considered, we do not consider nitrification process as a global process explaining our observations.

5. Conclusions

This study shows that carbonate weathering intensity, as recorded by Ca + Mg concentrations in rivers and springs draining regions

underlain by pure carbonate lithologies, follows a relatively simple boomerang-like relationship with temperature. This relationship shows a maximum carbonate weathering intensity under temperate conditions. A similar pattern is observed for carbonate weathering intensity in large river systems deduced by the inversion of chemical composition.

The simple qualitative interpretation we propose to explain the boomerang relationship between carbonate weathering intensity and temperature relies on two competitive effects that both depend on temperature. This boomerang pattern results from a compromise between the dependence of equilibrium constants of the carbonate system in aqueous solution with temperature (decreases with T) and the production of soil CO_2 by ecosystems which depends on temperature (increases with T) and soil moisture.

This relationship presents some scatter, meaning that other parameters influencing carbonate weathering have to be taken into account at a regional scale. This first order study shows the strong sensitivity of carbonate weathering to environmental parameters and potentially to the actual global warming and change in land use and land cover. Given the fast response of carbonate weathering, there is a need for a better understanding and modeling of carbonate weathering processes at both local and global scales. Carbonate weathering is not only important as a major CO_2 consumption process, it is also a dominant control in determining water quality.

Overall, this study urgently calls for more investigation on carbonate weathering. Because carbonate weathering is a rapid process, it is able to respond quickly to short-term processes such as biological processes and is therefore a core mechanism of the Earth's Critical Zone that links biological, hydrological and geological processes. In response to global change, carbonate weathering is an interesting atmospheric CO_2 sink and a source of alkalinity to the ocean that is able to play a key role at the 100 years to 10,000 years timescales (Beaulieu et al., 2012).

Supplementary data to this article can be found online at https://doi.org/10.1016/j.chemgeo.2018.05.009.

Acknowledgement

Oleg Pokrovsky, Jacques Schott, Yves Goddéris, Julien Bouchez, Nicole Fernandez are thanked for their careful comments. We thank Matthiew Wimmick and Pamela Sullivan for constructive reviews. Funding for this work in Germany has been provided by German Science Foundation (DFG) through the Cluster of Excellence CLISAP2 (DFG Exec177, Universität Hamburg), and BMBF-project PALMOD (Ref 01LP1506C) through the German Ministry of Education and Science (BMBF) as Research for Sustainability initiative (FONA). JG thank the Institut Universitaire de France for financial support. This is IPGP contribution number 3943.

References

Bakalowicz, M., 2005. Karst groundwater: a challenge for new resources. Hydrogeol. J. 13 (1), 148–160.
Beaulieu, E., Goddéris, Y., Donnadieu, Y., Labat, D., Roelandt, C., 2012. High sensitivity of the continental-weathering carbon dioxide sink to future climate change. Nat. Clim. Chang. 2 (5), 346–349.
Berner, R.A., 1984. Sedimentary pyrite formation: an update. Geochim. Cosmochim. Acta 48 (4), 605–615.
Berner, E.K., Berner, R.A., 2012. Global Environment: Water, Air, and Geochemical Cycles. Princeton University Press.
Bluth, G.J., Kump, L.R., 1994. Lithologic and climatologic controls of river chemistry. Geochim. Cosmochim. Acta 58 (10), 2341–2359.
Brook, G.A., Folkoff, M.E., Box, E.O., 1983. A world model of soil carbon dioxide. Earth Surf. Process. Landf. 8 (1), 79–88.
Calmels, D., Gaillardet, J., Brenot, A., France-Lanord, C., 2007. Sustained sulfide oxidation by physical erosion processes in the Mackenzie River basin: climatic perspectives. Geology 35 (11), 1003–1006.
Calmels, D., Gaillardet, J., François, L., 2014. Sensitivity of carbonate weathering to soil CO_2 production by biological activity along a temperate climate transect. Chem. Geol. 390, 74–86.
Chiodini, G., Frondini, F., Cardellini, C., Granieri, D., Marini, L., Ventura, G., 2001. CO_2 degassing and energy release at Solfatara volcano, Campi Flegrei, Italy. J. Geophys. Res. Solid Earth 106 (B8), 16213–16221.
Corbel, J., 1959, March. Erosion en terrain calcaire (vitesse d'érosion et morphologie). In: Annales de geographie. vol. 68, no. 366. Armand Colin, pp. 97–120.
Drake, J.J., 1980. The effect of soil activity on the chemistry of carbonate groundwaters. Water Resour. Res. 16 (2), 381–386.
Drake, J.J., Wigley, T.M.L., 1975. The effect of climate on the chemistry of carbonate groundwater. Water Resour. Res. 11 (6), 958–962.
Dreybrodt, W., 1988. Processes in Karst Systems: Physics. Chemistry, and Geology. Springer, Berlin.
Dreybrodt, W., Lauckner, J., Zaihua, L., Svensson, U., Buhmann, D., 1996. The kinetics of the reaction $CO_2 + H_2O \rightarrow H^+ + HCO_3^-$ as one of the rate limiting steps for the dissolution of calcite in the system H_2O-CO_2 $CaCO_3$. Geochim. Cosmochim. Acta 60 (18), 3375–3381.
Ebelmen, J.J., 1845. Sur les produits de la décomposition des espèces minérales de la famille des silicates. In: Annales des Mines. vol. 7, no. 3. pp. 66.
Eisenlohr, L., Meteva, K., Gabrovšek, F., Dreybrodt, W., 1999. The inhibiting action of intrinsic impurities in natural calcium carbonate minerals to their dissolution kinetics in aqueous H_2O–CO_2 solutions. Geochim. Cosmochim. Acta 63 (7), 989–1001.
Evans, M.J., Derry, L.A., France-Lanord, C., 2004. Geothermal sources of alkalinity in the Narayani river system of central Nepal. Geochem. Geophys. Geosyst. 5 (8), 1–21.
Ferguson, P.R., Dubois, K.D., Veizer, J., 2011. Fluvial carbon fluxes under extreme rainfall conditions: inferences from the Fly River, Papua New Guinea. Chem. Geol. 281 (3), 283–292.
Floury, P., Gaillardet, J., Gayer, E., Bouchez, J., Tallec, G., Ansart, P., Koch, F., Gorge, C., Blanchouin, A., Roubaty, J.L., 2017. The potamochemical symphony: new progress in the high frequency acquisition of stream chemical data. Hydrol. Earth Syst. Sci. Discuss. 2017. http://dx.doi.org/10.5194/hess-2017-12.
Ford, D., Williams, P.D., 2013. Karst Hydrogeology and Geomorphology. John Wiley & Sons.
Gabrovšek, F., 2009. On concepts and methods for the estimation of dissolutional denudation rates in karst areas. Geomorphology 106 (1–2), 9–14.
Gaillardet, J., Dupré, B., Louvat, P., Allegre, C.J., 1999. Global silicate weathering and CO_2 consumption rates deduced from the chemistry of large rivers. Chem. Geol. 159 (1), 3–30.
Galy, A., France-Lanord, C., 1999. Weathering processes in the Ganges–Brahmaputra basin and the riverine alkalinity budget. Chem. Geol. 159, 31–60.
Garrels, R.M., Christ, C.L., 1965. Solutions, Minerals, and Equilibria.
Giusti, E.V., 1978. Hydrogeology of the Karst of Puerto Rico. vol. 1012 US Govt. Print. Off.
Goddéris, Y., Roelandt, C., Schott, J., Pierret, M.C., François, L.M., 2009. Towards an integrated model of weathering, climate, and biospheric processes. Rev. Mineral. Geochem. 70 (1), 411–434.
Goddéris, Y., Williams, J.Z., Schott, J., Pollard, D., Brantley, S.L., 2010. Time evolution of the mineralogical composition of Mississippi Valley loess over the last 10 kyr: climate and geochemical modeling. Geochim. Cosmochim. Acta 74 (22), 6357–6374.
Gombert, P., 2002. Role of karstic dissolution in global carbon cycle. Glob. Planet. Chang. 33, 177–184.
Gwiazda, R.H., Broecker, W.S., 1994. The separate and combined effects of temperature, soil pCO_2, and organic acidity on silicate weathering in the soil environment: formulation of a model and results. Glob. Biogeochem. Cycles 8 (2), 141–155.
Han, G., Liu, C.Q., 2004. Water geochemistry controlled by carbonate dissolution: a study of the river waters draining karst-dominated terrain, Guizhou Province, China. Chem. Geol. 204 (1), 1–21.
Hartmann, J., Lauerwald, R., Moosdorf, N., 2014. A brief overview of the GLObal RIver Chemistry Database, GLORICH. Procedia Earth aPlanet. Sci. 10, 23–27.
Hijmans, R.J., Cameron, S.E., Parra, J.L., Jones, P.G., Jarvis, A., 2005. Very high resolution interpolated climate surfaces for global land areas. Int. J. Climatol. 25 (15), 1965–1978.
Holland, H.D., 2003. The geologic history of seawater. In: Treatise on Geochemistry. 6. pp. 625.
Huh, Y., Tsoi, M.Y., Zaitsev, A., Edmond, J.M., 1998. The fluvial geochemistry of the rivers of Eastern Siberia: I. Tributaries of the Lena River draining the sedimentary platform of the Siberian Craton. Geochim. Cosmochim. Acta 62 (10), 1657–1676.
Ibarra, D.E., Moon, S., Caves, J.K., Chamberlain, C.P., Maher, K., 2017. Concentration–discharge patterns of weathering products from global rivers. Acta Geochim. 36 (3), 405–409.
Ilstedt, U., Nordgren, A., Malmer, A., 2000. Optimum soil water for soil respiration before and after amendment with glucose in humid tropical acrisols and a boreal mor layer. Soil Biol. Biochem. 32 (11-12), 1591–1599.
Jacobson, R.L., Langmuir, D., 1974. Controls on the quality variations of some carbonate spring waters. J. Hydrol. 23 (3–4), 247–265.
Jessen, S., Holmslykke, H.D., Rasmussen, K., Richardt, N., Holm, P.E., 2014. Hydrology and pore water chemistry in a permafrost wetland, Ilulissat, Greenland. Water Resour. Res. 50 (6), 4760–4774.
Karim, A., Veizer, J., 2000. Weathering processes in the Indus River Basin: implications from riverine carbon, sulfur, oxygen, and strontium isotopes. Chem. Geol. 170 (1), 153–177.
Katz, B.G., Catches, J.S., Bullen, T.D., Michel, R.L., 1998. Changes in the isotopic and chemical composition of ground water resulting from a recharge pulse from a sinking stream. J. Hydrol. 211 (1), 178–207.
Lasaga, A.C., 1984. Chemical kinetics of water-rock interactions. J. Geophys. Res. Solid Earth 89 (B6), 4009–4025.
Le Quéré, C., Raupach, M.R., Canadell, J.G., Marland, G., Bopp, L., Ciais, P., ... Friedlingstein, P., 2009. Trends in the sources and sinks of carbon dioxide. Nat. Geosci. 2 (12), 831–836.

Lerman, A., Wu, L., 2006. CO_2 and sulfuric acid controls of weathering and river water composition. J. Geochem. Explor. 88 (1), 427–430.
Li, S.L., Calmels, D., Han, G., Gaillardet, J., Liu, C.Q., 2008. Sulfuric acid as an agent of carbonate weathering constrained by $\delta^{13}C$ DIC: examples from Southwest China. Earth Planet. Sci. Lett. 270 (3), 189–199.
Lieth, H., 1975. Modeling the primary productivity of the world. In: Primary Productivity of the Biosphere. Springer, Berlin Heidelberg, pp. 237–263.
Maher, K., Chamberlain, C.P., 2014. Hydrologic regulation of chemical weathering and the geologic carbon cycle. Science 343 (6178), 1502–1504.
Meybeck, M., 1986. Composition chimique des ruisseaux non pollués de France. Sci. Géol. Bull. 39, 3–77.
Michard, G., 2002. Chimie des eaux naturelles. Principe de Géochimie des Eaux. Editions PUBLISUD.
Millot, R., Jérôme Gaillardet, J., Dupré, B., Allègre, C.J., 2003. Northern latitude chemical weathering rates: clues from the Mackenzie River Basin, Canada. Geochim. Cosmochim. Acta 67 (7), 1305–1329.
Negrel, P., Allègre, C.J., Dupré, B., Lewin, E., 1993. Erosion sources determined by inversion of major and trace element ratios and strontium isotopic ratios in river water: the Congo Basin case. Earth Planet. Sci. Lett. 120 (1–2), 59–76.
Oliver, L., Harris, N., Bickle, M., Chapman, H., Dise, N., Horstwood, M., 2003. Silicate weathering rates decoupled from the $^{87}Sr/^{86}Sr$ ratio of the dissolved load during Himalayan erosion. Chem. Geol. 201 (1), 119–139.
Parkhurst, D.L., Appelo, C.A.J., 1999. User's Guide to PHREEQC (Version 2): A Computer Program for Speciation, Batch-reaction, One-dimensional Transport, and Inverse Geochemical Calculations.
Perrin, A.S., Probst, A., Probst, J.L., 2008. Impact of nitrogenous fertilizers on carbonate dissolution in small agricultural catchments: implications for weathering CO_2 uptake at regional and global scales. Geochim. Cosmochim. Acta 72 (13), 3105–3123.
Petelet, E., Luck, J.M., Othman, D.B., Negrel, P., Aquilina, L., 1998. Geochemistry and water dynamics of a medium-sized watershed: the Hérault, southern France: 1. Organisation of the different water reservoirs as constrained by Sr isotopes, major, and trace elements. Chem. Geol. 150 (1), 63–83.
Pitman, J.I., 1978. Carbonate chemistry of groundwater from tropical tower karst in south Thailand. Water Resour. Res. 14 (5), 961–967.
Qin, J., Huh, Y., Edmond, J.M., Du, G., Ran, J., 2006. Chemical and physical weathering in the Min Jiang, a headwater tributary of the Yangtze River. Chem. Geol. 227 (1), 53–69.
Rasse, D.P., François, L., Aubinet, M., Kowalski, A.S., Walle, I.V., Laitat, E., Gérard, J.C., 2001. Modelling short-term CO_2 fluxes and long-term tree growth in temperate forests with ASPECTS. Ecol. Model. 141 (1), 35–52.
Raymond, P.A., Hartmann, J., Lauerwald, R., Sobek, S., McDonald, C., Hoover, M., ... Kortelainen, P., 2013. Global carbon dioxide emissions from inland waters. Nature 503 (7476), 355–359.
Rive, K., Gaillardet, J., Agrinier, P., Rad, S., 2013. Carbon isotopes in the rivers from the Lesser Antilles: origin of the carbonic acid consumed by weathering reactions in the Lesser Antilles. Earth Surf. Process. Landf. 38 (9), 1020–1035.
Romero-Mujalli, G., Hartmann, J., Börker, J., Gaillardet, J., Calmels, D., 2018. Ecosystem controlled soil-rock pCO_2 and carbonate weathering - Constraints by temperature and soil water content. Chem. Geol. http://dx.doi.org/10.1016/j.chemgeo.2018.01.030. (in press).
Roy, S., Gaillardet, J., Allegre, C.J., 1999. Geochemistry of dissolved and suspended loads of the Seine river, France: anthropogenic impact, carbonate and silicate weathering. Geochim. Cosmochim. Acta 63 (9), 1277–1292.
Sarazin, G., Ciabrini, J.P., 1997. Water geochemistry of three mountain streams from carbonate watersheds in the Southern French Alps. Aquat. Geochem. 3 (3), 233–265.
Seneviratne, S.I., Corti, T., Davin, E.L., Hirschi, M., Jaeger, E.B., Lehner, I., Teuling, A.J., 2010. Investigating soil moisture–climate interactions in a changing climate: a review. Earth Sci. Rev. 99 (3), 125–161.
Spence, J., Telmer, K., 2005. The role of sulfur in chemical weathering and atmospheric CO_2 fluxes: evidence from major ions, $\delta^{13}C$ DIC, and $\delta^{34}S$ SO_4 in rivers of the Canadian Cordillera. Geochim. Cosmochim. Acta 69 (23), 5441–5458.
Szramek, K., McIntosh, J.C., Williams, E.L., Kanduc, T., Ogrinc, N., Walter, L.M., 2007. Relative weathering intensity of calcite versus dolomite in carbonate-bearing temperate zone watersheds: carbonate geochemistry and fluxes from catchments within the St. Lawrence and Danube river basins. Geochem. Geophys. Geosyst. 8 (4).
Thomazo, C., Buoncristiani, J.F., Vennin, E., Pellenard, P., Cocquerez, T., Mugnier, J.L., Gérard, E., 2017. Geochemical processes leading to the precipitation of subglacial carbonate crusts at Bossons Glacier, Mont Blanc Massif (French Alps). Front. Earth Sci. 5, 70.
Torres, M.A., West, A.J., Li, G., 2014. Sulphide oxidation and carbonate dissolution as a source of CO_2 over geological timescales. Nature 507 (7492), 346–349.
Torres, M.A., Moosdorf, N., Hartmann, J., Adkins, J.F., West, A.J., 2017. Glacial weathering, sulfide oxidation, and global carbon cycle feedbacks. Proc. Natl. Acad. Sci. 114 (33), 8716–8721.
Van Bavel, C.H.M., 1951. A soil aeration theory based on diffusion. Soil Sci. 72 (1), 33–46.
Xu, Z., Liu, C.Q., 2007. Chemical weathering in the upper reaches of Xijiang River draining the Yunnan–Guizhou Plateau, Southwest China. Chem. Geol. 239 (1), 83–95.
Yoshimura, K., Nakao, S., Noto, M., Inokura, Y., Urata, K., Chen, M., Lin, P.W., 2001. Geochemical and stable isotope studies on natural water in the Taroko Gorge karst area, Taiwan—chemical weathering of carbonate rocks by deep source CO_2 and sulfuric acid. Chem. Geol. 177 (3), 415–430.
Zhong, J., Li, S.-L., Tao, F., Yue, F., Liu, C.-Q., 2017. Sensitivity of chemical weathering and dissolved carbon dynamics to hydrological conditions in a typical karst river. Sci. Rep. 7.

Global climate control on carbonate weathering intensity

Gaillardet, Jérôme; Calmels, Damien; Romero-Mujalli, Gibran; Zakharova, Elena; Hartmann, Jens

01 Nicholas Gubbins Page 3
9/7/2021 16:16

02 Nicholas Gubbins Page 3
9/7/2021 16:17

03 Nicholas Gubbins Page 3
9/7/2021 16:17

04 Nicholas Gubbins Page 3
9/7/2021 16:17

05 Nicholas Gubbins Page 5
9/7/2021 16:20

06 Nicholas Gubbins Page 5
9/7/2021 16:20

07 Nicholas Gubbins Page 6
9/7/2021 16:20

08 Nicholas Gubbins Page 6
9/7/2021 16:20

09 Nicholas Gubbins Page 6
9/7/2021 16:20